Implications of finite-size and surface effects on nanosize intercalation materials

M. N. Obrovac

Department of Physics, Dalhousie University, Halifax, Nova Scotia, Canada B3H 3J5

J. R. Dahn*

Department of Physics and Department of Chemistry, Dalhousie University, Halifax, Nova Scotia, Canada B3H 3J5

(Received 15 June 1999)

A Monte Carlo simulation of a two-dimensional lattice gas with free boundaries is used to study the effects of surface and size on the chemical potential-composition curves of intercalation compounds. In particular we are interested in electrochemically active nanosize lithium intercalation compounds. Both surface and size effects were found to modify the chemical potential versus composition behavior of our model. By the manipulation of grain size and surface energy it may be possible to fine tune a material's chemical potential versus composition behavior.

I. INTRODUCTION

As nanosized materials ($<$20 nm) becomes easier to produce they are finding applications in a wide variety of fields. This is because nanosized materials can have dramatically different properties than their bulk counterparts. In the field of energy storage materials the possibilities of nanosized materials are just becoming realized. Recently it has been shown that hydrogen adsorption in metal hydrides can be greatly enhanced if the metal hydrides are made nanosized.[1] In the lithium battery field, carbons containing nanosized pores have been considered as high capacity anode materials.[2] We have also shown that Sn anodes can be cycled reversibly if the Sn is made a nanosized component of a composite anode.[3] Nanocrystalline cathode materials are also presently being studied.[4–6] All the above materials have the common property that features in their voltage curves (or absorption curves for metal hydrides) become rounded off as the grain size becomes smaller. This is a well-known property of systems with finite size.[7–9] In addition, the chemical potential for absorption, intercalation, or alloying in some of the above systems changes with the grain size. This is consistent with surface effects that can change the chemical potential of phase transitions in the bulk.[10] As the grain size becomes smaller these surface effects ought to have greater importance.

Here a lattice gas model is used to study the consequences of surface and size effects in intercalation materials. In particular we are interested in lithium intercalation materials and thus the language of lithium batteries will be used.[11] Although there have been many previous studies on finite-size and surface effects,[7–10,12–17] notably in magnetic lattices, these studies have mostly concentrated on the temperature dependence of phase transitions at zero magnetic field whereas here we are interested in changes in the composition with the chemical potential (or in magnetic terminology the isothermal magnetization as a function of field). Furthermore, previous studies usually separate finite-size and surface effects by using periodic boundary conditions or semi-infinite lattices, respectively.[14] Studies that emulate real materials with all boundaries free are few and such studies

on antiferromagnetic systems are even fewer.[15] To complicate matters, it is well known that the Ising model and the lattice gas models are equivalent on an infinite lattice. Usually lattice gas models are transformed into an Ising lattice to take advantage of its symmetry. Unfortunately, the two models are not equivalent on lattices with all boundaries free. In fact, the lattice gas model with free boundaries is equivalent to the Ising model surrounded by spins that are all ''pinned'' in a particular direction.[16]

Some general features of a lattice gas with free boundaries can be extracted from the literature. Because of the finite size of the lattice no singularities can occur during phase transitions and we may expect a rounding of the peak in the differential capacity (the susceptibility in the language of magnetism).[17] In a finite system with periodic boundary conditions the maximum differential capacity peak height is related to the system size by

$$(-dx/dV)_{max} \sim L^d, \tag{1}$$

where L is the linear dimension of the lattice of dimension d.[17] There should also be a shift in the voltage of a phase transition which is size dependent:[17] $V_s \sim L^{-1}$. Wetting transitions on the lattice boundaries should also occur, as is observed in the well-studied case of an Ising lattice with free boundaries.[14,18] As the grain size of active materials becomes smaller these effects will increase in importance.

II. THEORY

In the typical electrochemical cell arrangement used to test lithium intercalation electrodes the intercalation electrode is the cathode and the anode is lithium metal. Both are separated from each other by an electrolyte in which lithium ions are mobile. The voltage V of the cell is related to the chemical potential μ of lithium in the cathode by the relation

$$V = -\frac{1}{ze}(\mu - \mu_0), \tag{2}$$

where z is the charge on the lithium ion and is equal to 1, e is the electronic charge, and μ_0 is the chemical potential of

the lithium metal anode. As the cell charges and discharges μ_0 does not change and by convention is taken to be zero. Thus Eq. (2) reduces to $V = -\mu/e$ where μ is measured in electron volts. The voltage profile (voltage versus composition curve) of the electrochemical cell described above is then just the negative of the chemical potential versus the composition.

The lattice gas model is well suited to modeling lithium intercalation materials, which have large diffusion coefficients and are in quasiequilibrium at room temperature.[11] We consider an $L \times L$ square lattice gas with free boundaries as a simple model of a nanosized intercalation material. Since many lithium intercalation compounds are layered, the choice of a two-dimensional model is not unreasonable for these systems. For simplicity, only nearest-neighbor interactions are considered here. The $d=2$ square lattice gas with only nearest-neighbor interactions on an infinite lattice is well understood. The energy of the lattice is

$$A_{(\infty)} = U \sum_{\langle i,j \rangle} n_i n_j + (E - \mu) \sum_i n_i, \quad (3)$$

where the n_i's are the lattice site occupation numbers, $\langle i,j \rangle$ sums over nearest-neighbor sites, U is the interaction energy between the atoms on the lattice, and E is the lattice binding energy. The occupation x of the lattice is defined by

$$x = \frac{1}{L^2} \sum_i n_i. \quad (4)$$

For attractive nearest-neighbor interactions (negative U) the $d=2$ square lattice gas undergoes a first-order phase transition when $v = \tanh(U/kT) < v_c = -0.440\,68\cdots$ and $\mu = 2U + E$.[19] For repulsive interactions when $v > -v_c$ an ordered state with $x = \frac{1}{2}$ is formed when $\mu > E$ and the lattice completely fills when $\mu > 4U + E$.[19]

For our finite model with free boundaries it must be further considered that the interaction energy and the lattice binding energy in nanosized materials will most likely be different on the surface than in the bulk. As an approximation the excess surface and binding energies are restricted only to sites on the first layer. The energy of the model is then

$$A = U \sum_{\langle i,j \rangle b} n_i n_j + U_s \sum_{\langle i,j \rangle s} n_i n_j + (E - \mu) \sum_i n_i + E_1 \sum_{\text{surface}} n_i, \quad (5)$$

where $\langle i,j \rangle b$ and $\langle i,j \rangle s$ are sums over nearest-neighbor bulk and surface sites, respectively, U and U_s are the interaction energies between bulk and surface lithium atoms, respectively, and E_1 is the excess surface lattice binding energy. In this study only the effects of different surface and bulk lattice binding energies are considered while the nearest-neighbor interaction energy is made constant throughout. Thus we set $U = U_s$.

Equation (5) can be used to create μ-E_1 ground-state phase diagrams by comparing the free energies of lattices in a basis set of probable ground-state configurations. The phase behavior of the ground state can be useful to understand phase changes that occur at finite temperatures. All diagrams made in this manner almost have center of inver-

sion symmetry. This is not surprising since if Eq. (5) is written in the form of an Ising model it is almost symmetric with respect to inversion about the point $\mu = 2U + E$, $E_1 = U/2$ except for a sum over the corner sites.[20]

The Monte Carlo method was used to model lattices at finite temperatures. Lattice configurations were generated with a simple Metropolis algorithm[21] in which one site at a time was updated for each Monte Carlo step (MCS). For lattices with $U > 0$, five thousand MCSs per site were used to initialize the lattice and expectation values of x were averaged over another hundred thousand MCSs/site. For lattices with $U < 0$ there are large fluctuations near the phase transition and values of x were averaged over a million MCSs/site. Each system was started as an empty lattice and the lattice was allowed to fill by slowly raising the chemical potential, typically in steps of 0.005–0.01 eV. After the lattice was filled the chemical potential was scanned in the opposite direction to check for hysteresis. No hysteresis between the two curves was observed for any simulation and the data from the curves in both directions was consolidated to improve statistics. Simulations were performed on 300-MHz personal computers and each lasted anywhere from 10 min to 10 h, depending on the lattice size.

III. LATTICE GAS WITH ATTRACTIVE INTERACTIONS

A. Ground-state properties

A basis set of four ground states was used for lattices with attractive interactions. The energies of the states are given below where the states are labeled by the occupation number on their surface and bulk (x, x_b):

$$A_{(00)} = 0, \quad (6a)$$

$$A_{(10)} = 4(L-1)(U + E - \mu + E_1), \quad (6b)$$

$$A_{(01)} = (L-2)[(l-2)(2U + E - \mu) - 2U], \quad (6c)$$

$$A_{(11)} = L[2(L-1)(U + 4E_1) + E - \mu]. \quad (6d)$$

The chemical potentials at the transitions between configurations are given by

$$\mu_{(00)(10)} = U + E + E_1, \quad (7a)$$

$$\mu_{(00)(01)} = E + 2U[1 - (L-2)^{-1}], \quad (7b)$$

$$\mu_{(00)(11)} = E + 2U(1 - L^{-1}) + 4E_1(L-1)/L^2, \quad (7c)$$

$$\mu_{(01)(10)} = E + 2U + 4(L^2 - 8K + 8)^{-1}[2LU - (L-1)E_1], \quad (7d)$$

$$\mu_{(01)(11)} = E + U[2 - (L-1)^{-1}] + E_1, \quad (7e)$$

$$\mu_{(10)(11)} = E + 2U[1 + (L-2)^{-1}]. \quad (7f)$$

Figure 1 shows the resulting μ-E_1 phase diagram of a 6 $\times 6$ lattice with $U = -2.5\,kT$. In the language of wetting phenomena the lines $(00)(10)$ and $(01)(11)$ correspond to prewetting transitions, $(10)(11)$ and $(00)(01)$ correspond to extraordinary transitions, and the $(00)(11)$ line is the ordinary transition.[14,18] The intersection of the $(00)(10)$ and $(10)(11)$
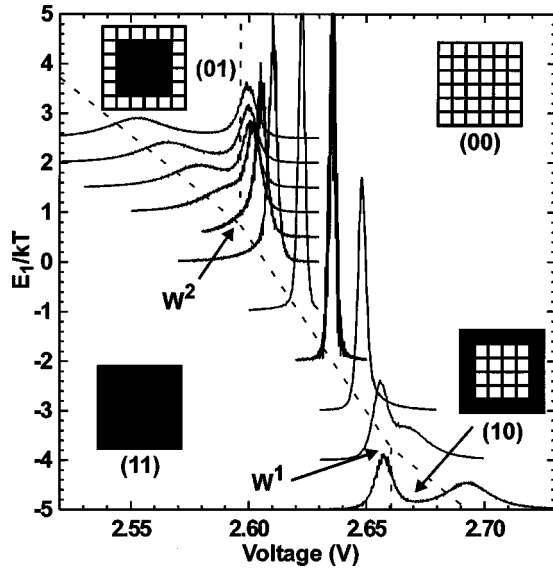
FIG. 1. The μ-E_1 ground-state phase diagram of a 6×6 lattice with attractive interactions. W^1 and W^2 are points of critical wetting. Differential capacity versus voltage curves obtained by Monte Carlo simulation are superimposed on the figure for comparison. All the differential capacity curves are plotted on the same scale, which is not shown in the figure, and are shifted in the vertical axis by E_1 ($U=-2.5$ kT, $E=-2.5$ eV).

lines and the (01)(11) and (00)(01) lines correspond to critical wetting transitions (labeled W^1 and W^2, respectively) and these occur at

$$W^1: \quad E_1 = U[1 + 2(L-2)^{-1}], \tag{8a}$$

$$W^2: \quad E_1 = U[(L-1)^{-1} - 2(L-2)^{-1}]. \tag{8b}$$

Because of the finite lattice size and the interaction between the bulk and surface atoms the chemical potential of the ordinary transition is dependent on E_1 and on L and the two wetting transitions do not occur at the same chemical potential as they do in a semi-infinite system.[18] The behavior of the infinite system is recovered in the limit $L \to \infty$ where both extraordinary transitions and the ordinary transition occur on the line $\mu = E + 2U$.

B. Monte Carlo simulations of lattices with attractive interactions

Figure 2 shows the voltage profiles for lattices with $L=6$, $U=-2.5$ kT and different values of E_1 calculated by Monte Carlo simulation. The differential capacity versus voltage is shown in Fig. 1 shifted by E_1 in the vertical direction. There is good agreement between the simulations and the ground-state phase diagram, which is drawn with dotted lines in the figure, however, the peaks at the ordinary transition are asymmetric. This asymmetry is caused by the surface sums in Eq. (5) and thus is strictly a surface effect. Qualitatively it can be described as thermal fluctuations between the (00) and (10) states or the (11) and (01) states. From Eq. (5) the curves should be symmetric (excepting the sum over the corners[20]) when $E_1 = U/2$.

Figure 3 shows the differential capacity versus voltage of lattices with $U=-2.5$ kT and $E_1=0$ for different values of
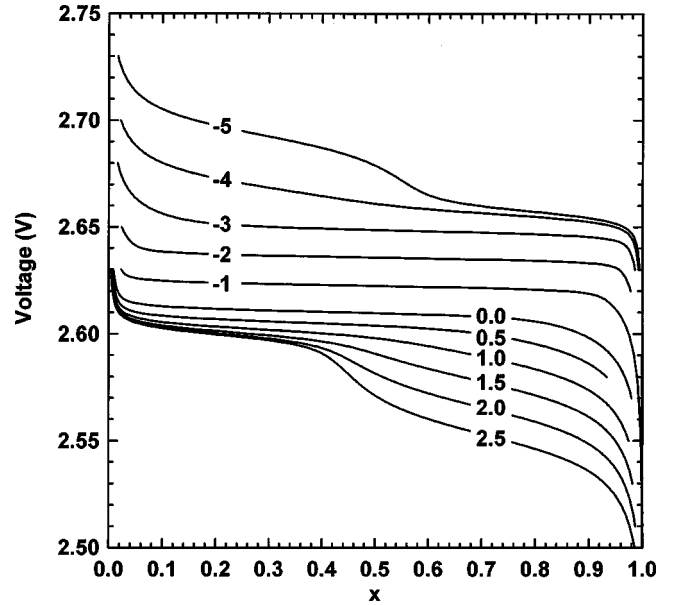

FIG. 2. Monte Carlo simulations of the voltage profiles of 6×6 lattices with attractive neighbor interactions and different values of the boundary energy E_1 (in units of kT) ($U=-2.5$ kT, $E=-2.5$ eV).

L. As predicted by Eq. (7c) the (00)(11) phase transition occurs at different voltages for different lattice sizes. The curves are also asymmetric, having a tail towards lower voltages [towards the (01) state] as discussed above. This rounding becomes larger as the lattice size becomes smaller and the number of surface sites becomes comparable to the bulk. The voltage profile is symmetric for $L=2$ since all the lattice sites are on the surface. Figure 4 shows the dependence of the peak height $(-dx/dV)_{max}$ and position V_{max} on the lattice size. Equation (7c) predicts a linear relationship between L and LV_{max}. There is excellent agreement with this predic-
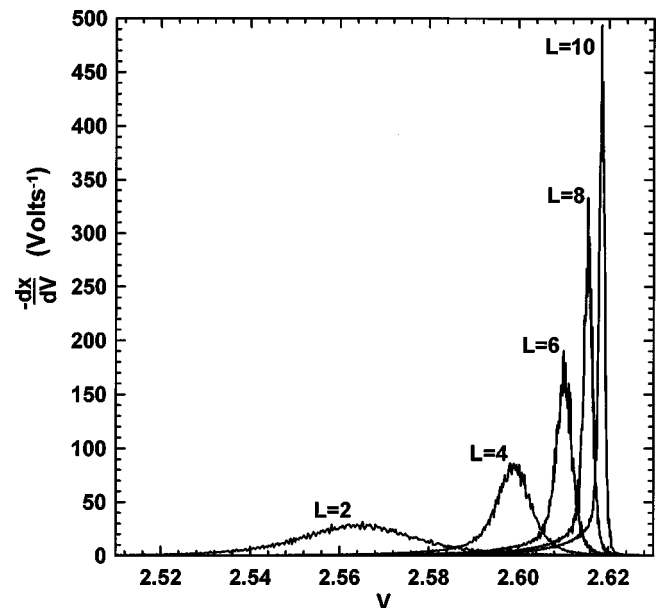

FIG. 3. Differential capacity versus voltage obtained by Monte Carlo simulation for different sized lattices with attractive neighbor interactions ($U=-2.5$ kT, $E_1=0$).
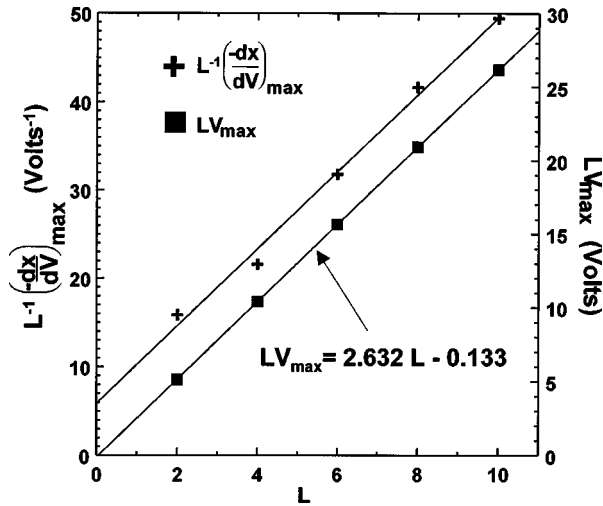
FIG. 4. $L^{-1}(-dx/dV)_{max}$ and LV_{max} versus L for lattices with attractive interactions ($U = -2.5$ kT, $E_1 = 0$).

tion in the figure. From Eq. (7c) the slope and intercept of the line should be $-(E + 2U) = 2.551$ eV and $2U = -0.1285$ eV, respectively, which are close to those values in the figure. Although Eq. (1) was derived for systems with periodic boundary conditions, $L^{-1}(-dx/dV)_{max}$ still appears to have a linear dependence on L for our system with fixed boundaries, but has a finite intercept at $L = 0$.

IV. LATTICE GAS WITH REPULSIVE INTERACTIONS

A. Ground-state properties

The ground-state properties of the finite lattice with repulsive interactions are more difficult to derive than in the case of attractive interactions since a larger number of ground states are possible. To model the ground-state properties an 8×8 lattice was chosen with $U = 10$ kT and $E = -2.5$ eV. The lattice was separated into three regions: the surface layer, the subsurface layer, and the remainder of the sites, being the core. These three regions could either be independently empty, full, or in the half full ordered state. In addition the corners of all three regions could all be independently full or empty. A computer program was used to determine the lowest energy state from all the permutations of possible configurations while the voltage was scanned. The resulting phase diagram is shown in Fig. 5.

Although the diagram appears complicated, the phase changes are intuitive. For example, going from point A to point B at the large attractive boundary potential of $E_1 = -40$ kT, the lattice first becomes alternately filled on the surface which has a higher binding energy than the bulk. The sites are filled alternately to avoid repulsive neighbor interactions. As the voltage is lowered the remaining surface sites all become filled and then the core sites are alternately filled. The subsurface layer remains empty because of the repulsive interactions from the filled surface sites. As the voltage is further lowered the subsurface layer alternately fills, save two corner sites which remain empty since they have two filled nearest-neighbor surface sites as opposed to the other subsurface sites which only have one each. The subsurface corners fill as the voltage is lowered below two volts. Now all the sites have four nearest neighbors and are equivalent,
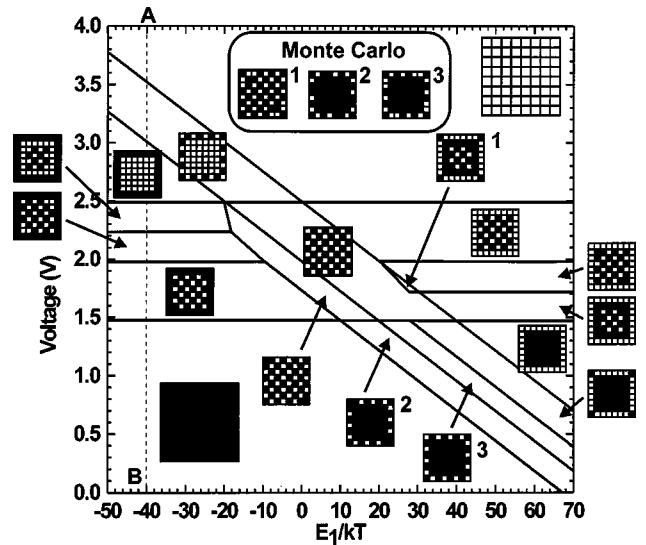

FIG. 5. Ground-state μ-E_1 phase diagram of an 8×8 lattice with repulsive neighbor interactions ($U = 10$ kT, $E = -2.5$ eV). The numbered phases did not occur in the Monte Carlo simulations. This is because of the limited basis set used to calculate the ground-state phase diagram. Phases obtained by Monte Carlo simulation at regions near the numbered phases are shown in the inset.

so the next phase has all sites filled. Similar arguments as the above can be used to explain all the phases in the diagram. The phases labeled 1, 2, and 3 were not observed in the Monte Carlo simulations. Instead phases with a frustrated surface layer were observed near the regions of phases 1, 2, and 3 which were not included in the limited basis set used to calculate the ground states. These phases are shown in the inset in Fig. 5.
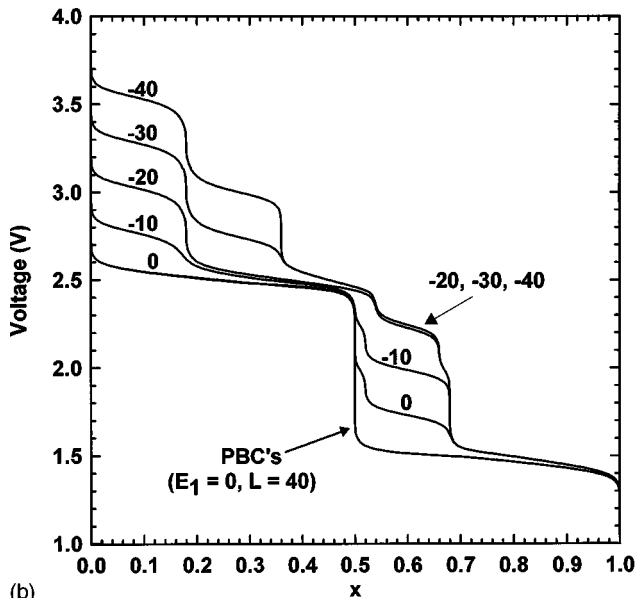
B. Monte Carlo simulations of lattices with repulsive interactions

Figures 6(a) and (b) show the voltage profiles for lattices with $L = 6$, $U = 10$ kT, and different values of E_1 calculated by Monte Carlo simulation. As predicted by the ground-state phase diagram, the voltage profiles of lattices with finite size have a number of plateaus corresponding to the different phase regions. Figure 7 shows the differential capacity curves of these lattices superimposed on the ground-state phase diagram. The results are in good agreement, even at large values of E_1 where phases appear that were not included in the basis set of the ground-state calculation. In Fig. 8 the voltage profiles for lattices with $L = 6$ and a smaller repulsive interaction of 5 eV is plotted for different values of E_1. The plateaus in this plot are more rounded and less defined than in Fig. 6. Despite this the surface lattice energy still has a large effect on the voltage curves.

Figure 9 shows voltage profiles of different size lattices with $U = 10$ kT and $E_1 = 0$ kT. The plateaus due to the various transitions change in capacity as the number of surface sites becomes comparable to the bulk. As with the case of attractive interactions there is also a change in the voltage of the various plateaus with the lattice size, although it is difficult to see on the scale of the figure. Figure 10 shows the differential capacity versus voltage for the order-disorder transition near 2.5 V. As the lattice size decreases the peak in
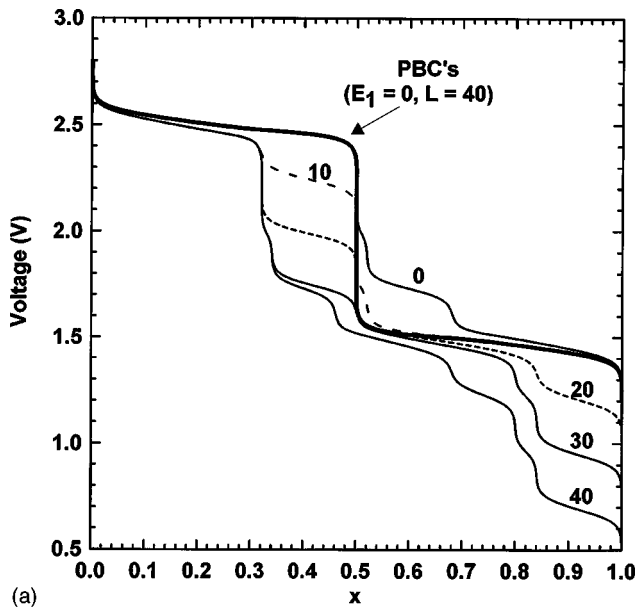
(a)

(b)

FIG. 6. Voltage profiles obtained by Monte Carlo simulation for 10×10 lattices with repulsive neighbor interactions and with (a) positive and (b) negative values of the surface lattice energy E_1 ($U = 10$ kT, $E = -2.5$ eV). For comparison the voltage curve of a 40×40 lattice with periodic boundary conditions is also shown.

the second-order transition becomes smaller and disappears for $L = 2$. To explain this behavior we note that the broad peak for the $L = 2$ lattice corresponds to the filling of a non-interacting lattice gas whereas in the infinite case there is frustration during the filling of the lattice which is released at the second-order transition. Finite lattices with $L > 2$ represent an intermediate case. These lattices have a large fraction of surface sites that have less nearest neighbors than those in the bulk. This means the probability for frustration is less in these lattices, making the second-order peak smaller than for the infinite case.

V. REAL FINITE-SIZE SYSTEMS

There are presently very few examples of nanosize storage materials that can be compared to the above model. This
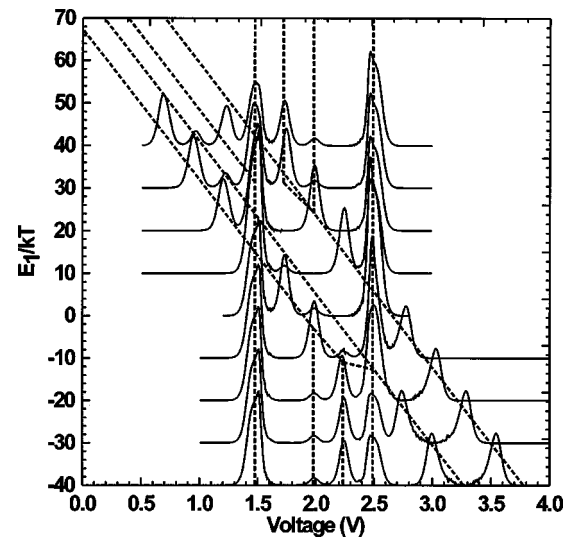

FIG. 7. Differential capacity versus voltage obtained by Monte Carlo simulation for 10×10 lattices with repulsive interactions and different values of E_1. The curves are all plotted on the same scale (not shown in the figure), but are shifted in the vertical axis by E_1. The ground-state phase diagram (Fig. 5) is superimposed on the figure for comparison ($U = 10$ kT, $E = -2.5$ eV).

is bound to change since more nanosized storage materials are starting to appear in the literature.[1–6] The above results can be used to predict the behavior of future materials, keeping in mind that real materials will probably have a rough surface with a distribution of grain sizes, interaction energies, and site energies. Conceivably, independent adjustment of both L and E_1 could be possible in real materials and could be used to effectively tune the voltage profile of the material. L is simply controlled by modification of the grain size while E_1 could be modified by encapsulating the grains in different matrix materials or by chemically treating the surface of the grains.

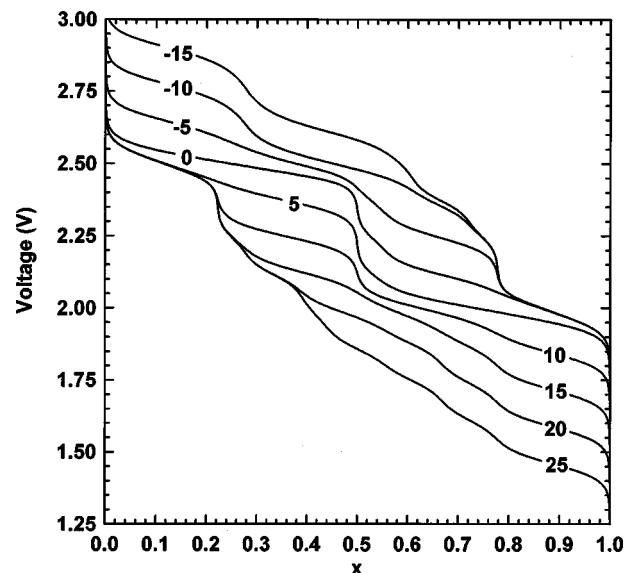For systems with attractive interactions and without sur-

FIG. 8. Voltage profiles obtained by Monte Carlo simulation for 10×10 lattices with repulsive neighbor interactions and different values of the surface lattice energy E_1 ($U = 5$ kT, $E = -2.5$ eV).
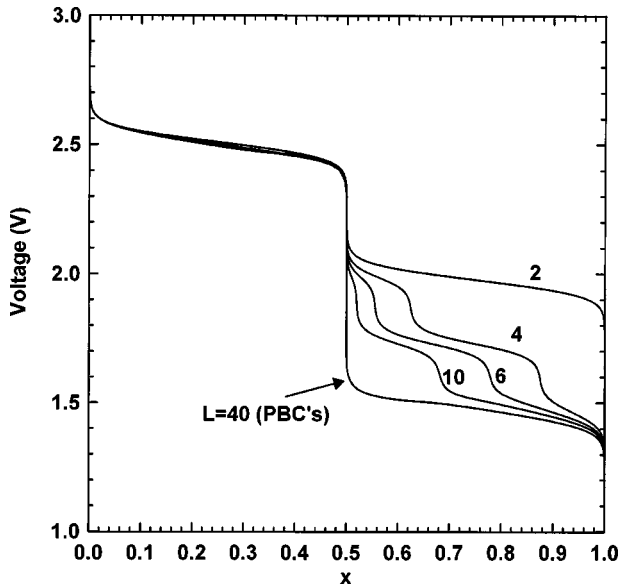
FIG. 9. Voltage profiles obtained by Monte Carlo simulation for different sized lattices with repulsive neighbor interactions and a negative surface energy of $E_1 = 0$ kT ($U = 10$ kT, $E = -2.5$ eV). For comparison, the voltage curve of a 40×40 lattice with periodic boundary conditions is also shown.

face wetting Eq. (7c) predicts that the difference in voltage between the phase transition in the finite-size system and the first-order phase transition in a system of infinite size will be

$$\Delta V_{\text{max}} = \frac{2U}{L} + 4E_1 \frac{(L-1)}{L^2}. \tag{9}$$

Typically, the voltage of a lithium test cell is measured to within a microvolt during cycling. However, because of diffusion, kinetic, and Ohmic effects only changes of about a
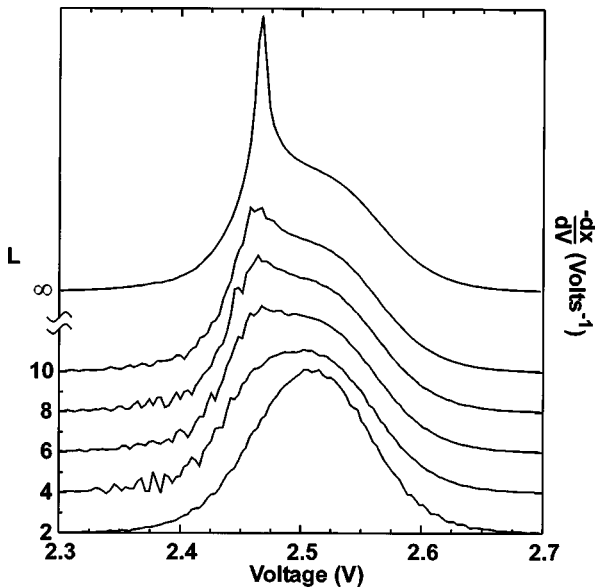

FIG. 10. Differential capacity versus voltage obtained by Monte Carlo simulation for lattices with repulsive interactions and different lattice size. The plots are shifted on the vertical axis by L. The infinite lattice is approximated by a 40×40 lattice with periodic boundary conditions ($U = 10$ kT, $E = -2.5$ eV, $E_1 = 0$ kT).

millivolt are observable in practice. Thus, assuming U is on the order of kT, $E_1 = 0$ and the Li-Li nearest-neighbor distance is about 0.2 nm, finite-size effects can be observed for grain sizes below 10 nm. However, these effects would be very small. In order to change the voltage of the (00)(11) phase transition significantly (by tenths of a volt) materials would have to have grain sizes less than 1 nm and $|U|$ or $|E_1|$ on the order of 10 kT. Larger effects could be expected for the prewetting transitions. For example, the (00)(10) transition occurs at $-(U+E_1)/e$ volts above the bulk transition voltage regardless of the system size. This transition will become observable when the capacity of the surface sites becomes measurable.

For systems with repulsive interactions the change in the voltages of the phase transitions caused by lattice size is also small. However, the surface transitions should occur at significantly different voltages than in the bulk and should be observable when the capacity of the surface and subsurface sites becomes measurable. For instance, in the present model of a square lattice if a site on the surface is surrounded by n filled neighbors it will be filled when the voltage is approximately $-(nU+E+E_1)/e$ whereas the bulk will have two plateaus at $-E/e$ and $-(E+4U)/e$ volts.

Although, as previously mentioned, we are not aware of any suitable measurements of the voltage composition behavior of nanosized intercalation systems to compare with our model, lithium intercalation into certain hydrogen-containing carbons provides an example in which finite-size effects can be observed.[2] However, the lithium interactions are slightly different than those used in the present model.[22] These carbons are made up of carbon sheets about 30 Å across with hydrogen atoms bonded to the carbons at the edges of the sheets.[2] When lithium is intercalated in this material it can either reside in the middle of a carbon hexagon in the bulk of the sheet where the Li-Li interaction is repulsive or bind to an edge carbon atom.[22] The binding energy of lithium to the edge carbons is greater than the sites in the bulk of the sheet by about 0.23 eV.[2] This corresponds to the case where $E_1 < 0$ and $U > 0$. However the surface-surface, surface-bulk, and bulk-bulk lithium neighbor interactions are probably quite different from each other. The surface-surface interaction may even be attractive.[22] Nevertheless, the contributions to the voltage curve from the edge and bulk sites can easily be differentiated although considerable hysteresis is associated with the filling of the surface sites.

VI. CONCLUSION

The effect of finite-size and of surface effects on intercalation materials have been studied by a square finite lattice-gas model. Particular emphasis was given to electrochemically active lithium intercalation compounds although the results should equally apply to other intercalation systems in which diffusion is fast enough to bring about quasiequilibrium. In the case of attractive nearest-neighbor interactions both surface effects and lattice size affected voltage profiles. Size effects cause differential capacity peaks to become rounded while surface effects modify the voltage at which they occur. Wetting transitions can also occur at the surface which cause additional peaks in the differential capacity

curves. The voltage of these peaks can be significantly different than the first-order transition in the bulk.

In a square lattice with repulsive interactions the filling of the surface and subsurface layers occur in many steps and can have a large effect on the voltage profile if the system is made small enough so that the number of surface sites becomes comparable to the bulk. In real materials in which there are many different kinds of surface sites these steps will probably be smeared out. However, the voltage of the surface and subsurface sites can be significantly different than the bulk and should be easy to observe if the particles are made small enough to measure the capacity of the surface sites. Further investigation is needed to study these effects. A better understanding of surface and size effects may lead to materials in which the voltage profiles can be modified by the manipulation of the grain size and surface energy.

---

*Author to whom correspondence should be addressed.

[1] L. Zaluski, A. Zaluska, and J. O. Ström-Olsen, J. Alloys Compd. **253-254**, 70 (1997).

[2] T. Zheng, W. R. McKinnon, and J. R. Dahn, J. Electrochem. Soc. **143**, 2137 (1996).

[3] O. Mao, R. L. Turner, I. A. Courtney, B. D. Fredericksen, M. I. Buckett, L. J. Krause, and J. R. Dahn, Electrochem. Solid-State Lett. **2**, 3 (1999).

[4] D. Xiao, P. R. Strutt, M. Benaissa, H. Chen, and B. H. Kear, Nanostruct. Mater. **10**, 1051 (1998).

[5] David E. Reisner, Alvin J. Salkind, Peter R. Strutt, and T. Danny Xiao, J. Power Sources **65**, 231 (1997).

[6] J.-H. Choy, D.-H. Kim, C.-W. Kwon, S.-J. Hwang, and Y.-I. Kim, J. Power Sources **77**, 1 (1999).

[7] M. E. Fisher, in *Proceedings of the 1970 Enrico Fermi Summer School on Critical Phenomena, Villa Monastero, Yarenna sul Lago di Como, Italy* (Academic, New York, 1971), p. 1.

[8] D. P. Landau, Phys. Rev. B **13**, 2997 (1976).

[9] Arthur E. Ferdinand and Michael E. Fisher, Phys. Rev. **185**, 185 (1969).

[10] H. Nakanishi and M. E. Fisher, J. Chem. Phys. **78**, 3279 (1983).

[11] W. R. McKinnon and R. R. Haering in, *Modern Aspects of Electrochemistry No. 15*, edited by R. E. White, J. O'M. Bockris, and B. E. Conway (Plenum, New York, 1983).

[12] K. Binder, Physica (Amsterdam) **62**, 508 (1972).

[13] D. P. Landau, Phys. Rev. B **14**, 255 (1976).

[14] H. W. Diehl in *Phase Transitions and Critical Phenomena*, edited by C. Domb and J. L. Lebowitz (Academic, New York, 1986), Vol. 10, p. 76.

[15] E. V. Albano, K. Binder, Dieter W. Heermann, and W. Paul, Surf. Sci. **223**, 151 (1989).

[16] Micheal E. Fisher and Arthur E. Ferdinand, Phys. Rev. Lett. **19**, 169 (1967).

[17] Micheal E. Fisher and A. Nihat Berker, Phys. Rev. B **26**, 2507 (1982).

[18] Hisao Nakanishi and Micheal E. Fisher, Phys. Rev. Lett. **49**, 1565 (1982).

[19] M. F. Sykes and Micheal E. Fisher, Physica (Amsterdam) **28**, 919 (1962).

[20] Equation (5) can be written equivalently in the form of an Ising model surrounded completely by spins pinned downward:

$$A = -J\sum_{\langle i,j\rangle b} \sigma_i\sigma_j - J_s\sum_{\langle i,j\rangle s}\sigma_i\sigma_j - H\sum_i \sigma_i - H_1\sum_{\text{surface}}\sigma_i + J\sum_{\text{surface}}\sigma_i$$

$$+ J\sum_{\text{corners}}\sigma_i + E_{\text{mo}},$$

where $\sigma_i = 2n_i + 1$. Comparison to Eq. (5) gives

$$J = -\frac{U}{4}, \quad J_s = -\frac{U_s}{4}, \quad H = (\mu - E)/2 - U, \quad H_1 = [(U - U_s) - E_1]/2,$$

$$E_{\text{mo}} = 2J[L(L-1)+2] + 4J_s(L-1) - HL^2 - 4H_1(L-1).$$

For the case $U = U_s$ and $J = J_s$ the equation in Ising formalism is almost symmetric with respect to inversion about the point $H = 0$ and $H_1 = J(\mu = 2U + E, E_1 = U/2)$ except for the sum over the corner sites.

[21] N. Metropolis, A. W. Rosenbluth, M. N. Rosenbluth, A. H. Teller, and E. Teller, J. Chem. Phys. **21**, 1087 (1953).

[22] P. Papanek, M. Radosavljevic, and J. E. Fischer, Chem. Mater. **8**, 1519 (1996).